Virtual Satellite Construction and Application for Image Classification



2014 IOP Conf. Ser.: Earth Environ. Sci. 17 012084

(http://iopscience.iop.org/1755-1315/17/1/012084)

# Virtual Satellite Construction and Application for Image Classification

**WG SU[1,2,3], FZ SU[2*], CH ZHOU[2]**

[1]Key Laboratory of Coastal Zone Environmental Processes, Yantai Institute of Coastal Zone Research(YIC), Chinese Academy of Sciences(CAS); Shandong Provincial Key Laboratory of Coastal Zone Environmental Processes, YICCAS, Yantai Shandong 264003, P. R. China;

[2]LREIS, Institute of Geographic Sciences and Natural Resources Research, CAS, Beijing 100101, China;

[3]University of Chinese Academy of Sciences, Beijing 100049, China

Corresponding author: sufz@ lreis.ac.cn.

**Abstract:** Nowadays, most remote sensing image classification uses single satellite remote sensing data, so the number of bands and band spectral width is consistent. In addition, observed phenomenon such as land cover have the same spectral signature, which causes the classification accuracy to decrease as different data have unique characteristic. Therefore, this paper analyzes different optical remote sensing satellites, comparing the spectral differences and proposes the ideas and methods to build a virtual satellite. This article illustrates the research on the TM, HJ-1 and MODIS data. We obtained the virtual band $X_0$ through these satellites' bands combined it with the 4 bands of a TM image to build a virtual satellite with five bands. Based on this, we used these data for image classification. The experimental results showed that the virtual satellite classification results of building land and water information were superior to the HJ-1 and TM data respectively.

## 1. Introduction

Information on the spatial distribution of land use or land cover is important for various tasks, including land-management planning and broader environmental monitoring and policy applications [1-2]. Therefore, it is necessary to monitor periodically the classification of land cover. Relying on the specialized skills of trained personnel, such information is generally acquired via manual input or prior knowledge and it often incurs high costs [3]. However, the development of remote sensing technology has simplified remote sensing image classification.

Although there are advantages to single source remote sensing data, the joint application of multisource data is the primary trend in current remote sensing development and multisource data combinations are believed to offer enhanced capabilities for the classification of target surfaces [4]. Over recent decades, numerous studies have shown the classification efficacy of multisource remote sensing data. A change detection approach based on independent component analysis has been proposed, which was used to separate change information in independent components by reducing the 2nd and higher order dependences in multi-temporal images [5]. Principal component analysis and hybrid classification methods have been used to detect land-use changes in an urban environment

using multi-temporal and multi-sensor data [6]. Multi-temporal Moderate Resolution Imaging Spectroradiometer (MODIS) data have been used for land cover classification [7-8]. Low resolution data, such as the Advanced Very High Resolution Radiometer (AVHRR) data collected by National Oceanic and Atmospheric Administration (NOAA) satellites, have been used to perform large-scale land cover classification and environmental detection because of their high temporal resolution and wide spatial coverage [7]. They have also been combined with thematic mapper (TM) data or aerial photos for land-use analysis [9-10]. These studies were based on multi-temporal or multisource data from a single satellite. The classification was finalised by fusion of multisource data or based on existing satellite bands. However, there were errors in image classification and other issues because the limited band numbers and fixed bandwidth meant that different land cover had similar spectral characteristics.

In this paper, we analysed the spectral differences of distinct optical remote sensing satellites and established relationships between different satellite bands. We obtained a virtual band through band operation and combined with Landsat data, established a virtual satellite. Based on this, we used the maximum likelihood method on the virtual satellite data for image classification in the experimental area and compared the results with the classification based on TM and HJ-1 data.

## 2. Methodology

Different satellites have different physical parameters, especially with regard to limited satellite bands and fixed bandwidth, which generate the same spectrum for different land cover (figure 1).

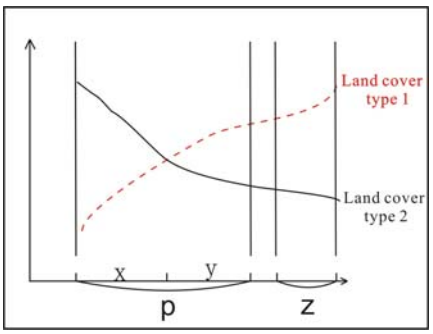


**Figure 1.** Spectrum of land cover

We performed research on two different land cover (refer to figure 1); they each exhibit different reflectance for a fixed band *p* but it is difficult to distinguish them on a band *p* image. Conversely, if the fixed band *p* is divided into bands *x* and *y*, the spectral characteristics of reflectance of the two land cover are different in these two bands and therefore, they can be distinguished. However, the existing satellite band cannot be changed. If a new satellite band *z* is used in the band operation between different satellites and combined with band *p* to establish a new satellite, then the two land cover can be distinguished using the new satellite data. Thus, band *z* is called a virtual band and the new satellite comprising band *p* and *z* is called a virtual satellite. In summary, this paper presents a method to construct a virtual band and a virtual satellite, as shown in figure 2.

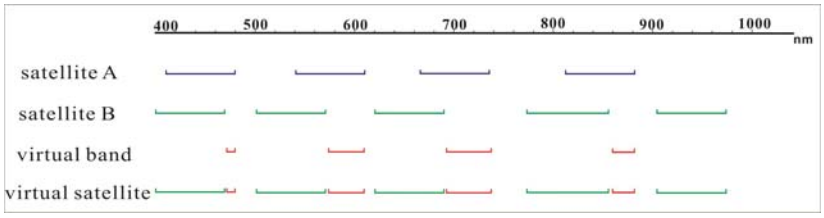


**Figure 2.** Virtual satellite construction

First, we obtain band coefficients by (1).

$$M \times \begin{pmatrix} A_{11} & \cdots & A_{1n} \\ \vdots & \ddots & \vdots \\ A_{m1} & \cdots & A_{mn} \end{pmatrix} - N \times \begin{pmatrix} B_{11} & \cdots & B_{1n} \\ \vdots & \ddots & \vdots \\ B_{m1} & \cdots & B_{mn} \end{pmatrix} = \begin{pmatrix} C_{11} & \cdots & C_{1n} \\ \vdots & \ddots & \vdots \\ C_{m1} & \cdots & C_{mn} \end{pmatrix} \quad (1)$$

$M$ and $N$ are band coefficients. $A_{mn}$ and $B_{mn}$ are the reflectance values of the same object in the same area using the same bands of satellite $A$ and satellite $B$. $C_{mn}$ is the reflectance value of different bandwidths between satellite $A$ and satellite $B$. We can obtain the band coefficients $M$ and $N$ through calculation of different objects. Then, we derive the reflectance $X_{i,j}$ of the virtual band $X_0$ (2).

$$X_{i,j} = M \times A_{i,j} - N \times B_{i,j} \quad (2)$$

The virtual band will be combined with satellite $B$ to build a virtual satellite.

## 3. Data

The study area was focused on the southern Luannan coastal plain in Liaoning Province of China, located between 39°17'–39°22'N and 118°27'–118°36'E. The main land cover are building land, water, rice, corn, forest lawn and vegetable plots.

A cloud-free and corrected Landsat5 image with 30-m spatial resolution acquired on 27 September 2007 and an HJ-1 satellite image with 30-m spatial resolution and a MODIS image with 1000-m spatial resolution acquired on 28 September 2007 were selected and downloaded from the USGS, China Centre for Resources Satellite Data and NASA, respectively.

The TM and HJ-1 data were converted to reflectance by radiometric calibration, the MODIS band 9 data resampling was processed using software and a relationship between the datasets established. The band coefficients were obtained by (1), in which $M = -0.462$ and $N = -1.5589$. Virtual band $X_0$ was derived by (2), according to the band coefficients and combined with Landsat to construct the virtual satellite.

## 4. Results and discussion

The results of the image classification in the study area for the TM image, HJ-1 satellite image and the virtual satellite image are presented in figure 3(a), 3(b) and 3(c), respectively. Generally, the three classification results are consistent with the land cover of the study area.

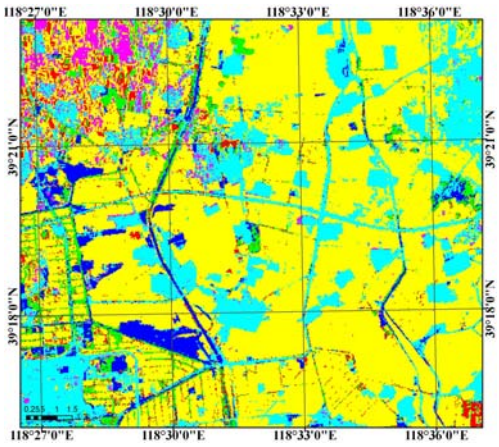


(a)

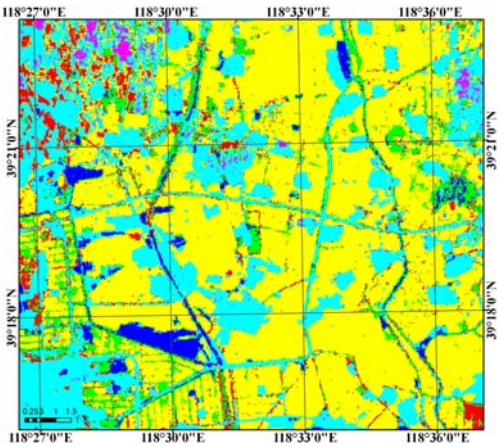


(b)

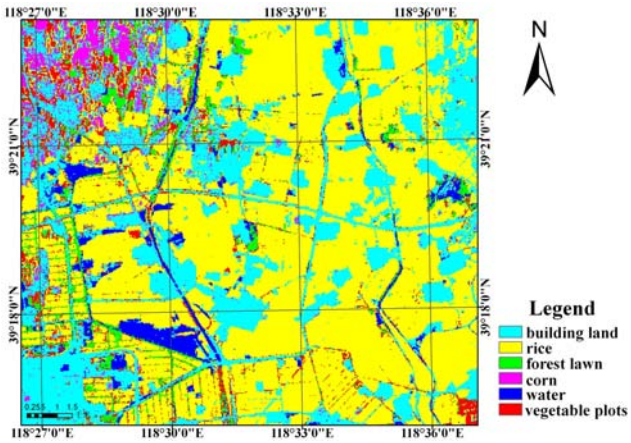


(c)

**Figure 3.** Classification results

To evaluate the accuracy of the classification results, we selected 200 samples randomly to create a confusion matrix. The overall accuracy and Kappa coefficient were calculated, together with the producer's accuracy and user's accuracy of land cover (table 1). The overall accuracy of the TM classification result is 70.5% and the Kappa coefficient is 0.4804, whereas for HJ-1 they are 70% and 0.5208 and for the virtual satellite they are 69.5% and 0.4981.

**Table 1.** Classification accuracy

| | TM | HJ-1 | virtual satellite |
|---|---|---|---|
| Overall accuracy | 70.5% | 70% | 69.5% |
| Kappa coefficient | 0.4804 | 0.5208 | 0.4981 |
| | producer's accuracy | producer's accuracy | producer's accuracy |
| building land | 80.65% | 87.10% | 90.32% |
| water | 40.00% | 40.00% | 40.00% |
| rice | 86.55% | 84.03% | 84.87% |
| corn | 14.29% | 0.00% | 0.00% |
| forest lawn | 21.05% | 36.84% | 15.79% |
| vegetable plots | 11.11% | 11.11% | 11.11% |
| | user's accuracy | user's accuracy | user's accuracy |
| building land | 55.56% | 49.09% | 50.00% |
| water | 85.71% | 100.00% | 100.00% |
| rice | 81.10% | 90.91% | 88.60% |
| corn | 25.00% | 0.00% | 0.00% |
| forest lawn | 36.36% | 49.09% | 33.33% |
| vegetable plots | 16.67% | 20.00% | 9.09% |

The Kappa coefficient of the HJ-1 satellite is the highest of the three and that of the virtual satellite is higher than the TM. Although the overall classification accuracy of the virtual satellite is lower than that of both the TM and HJ-1, the producer's accuracy and user's accuracy of the virtual satellite for the classification of building land are 3.22% and 0.91% higher than HJ-1. The user's accuracy of the virtual satellite for water classification is 14.29% higher than the TM. This shows that the virtual satellite is superior to the HJ-1 in classifying building land (figure 4) and better than TM in classifying water classification (figure 5).

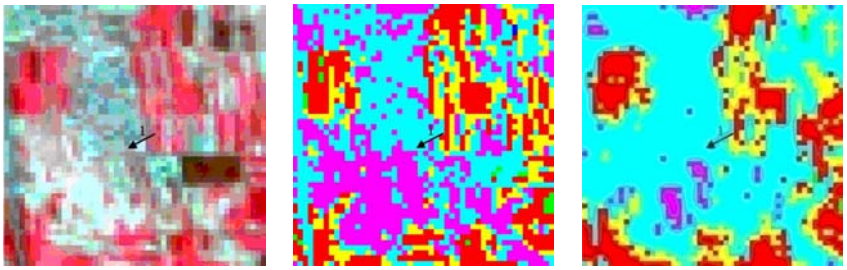

(a) (b) (c)

**Figure 4.** Classification result of virtual satellite and HJ-1 for building land

From the false colour image (figure 4(a)), it can be seen that the classification result of the HJ-1 satellite (figure 4(c)) generates a misclassification phenomenon, as indicated by the arrows; here, corn is mixed with building land. However, the virtual satellite produces a better classification result (figure 4(b)), which ensures the accuracy of the image classification.

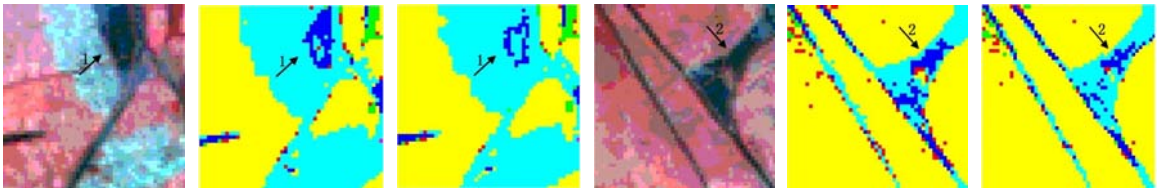

(a) (b) (c) (d) (e) (f)

**Figure 5.** Classification result of virtual satellite and TM for water

The TM classification results (figure 5(c), 5(f)) generate a misclassification phenomenon. The classification results only distinguish the boundary of the water (figure 5(c)). In figure 5(f), compared with the original false colour image, although the character of the water classification result is similar, a little water information has been missed. Most of the water is classified in the result of the virtual satellite, which is superior to the TM classification result.

## 5. Conclusions

In this study, we obtained a virtual band $X_0$ through spectral analysis based on TM, HJ-1 and MODIS data and combined it with Landsat data to construct a virtual satellite. Then, unsupervised classification was used to categorize the TM, HJ-1 and virtual satellite data in the experimental area. The results indicate that the building land classification by the virtual satellite is superior to that of HJ-1 and that the water classification by the virtual satellite is better than that of the TM.

Although the accuracy of the classification of certain feature shows that the virtual satellite is better than the conventional satellites, the overall accuracy is not the highest because too few band numbers are used and the spectral information is insufficient. Consequently, to improve the accuracy of remote sensing image classification, the number of bands should be increased and spectral information enriched in future constructions of virtual satellites.

## Acknowledgements

This research was supported by the National Key Technology R&D Program of China (Project number: 2011BAH23B04) and the National High Technology Research and Development Program of China (863 Program) (Project number: 2007AA092202).

## References

[1] Cihlar J 2000 Land cover mapping of large areas from satellites: status and research priorities *International Journal of Remote Sensing* **21**:1093-1114

[2] Park M H and Stenstrom M K 2008 Bayesian network application for urban land use classification *Journal of Environmental Management* **86**:181-192

[3] Wisdom M Dlamini 2011 Application of a Bayesian network for land-cover classification from a Landsat 7 ETM+ image *International Journal of Remote Sensing* **32**:6569-6586

[4] Benediktsson J A 1999 Classification of multisource and hyperspectral data based on decision fusion *IEEE Transactions on Geoscience and Remote Sensing* **37**:1367-1377

[5] Zhong J and Wang R 2005 Multi-temporal remote sensing change detection based on independent component analysis *International Journal of Remote Sensing* **27**:2055-5061

[6] Deng J S, Wang K, Deng Y H and Qi G J 2008 PCA-based land-use change detection and analysis using multitemporal and multisensor satellite data *International Journal of Remote Sensing* **29**:4823-4838

[7] Bagan Hasi, Wang Qinxue, Masataka Watanabe, Yang Yonghui and MA Jianwen 2005 Land Cover Classification from MODIS EVI Times-series Data Using SOM Neural Network *International Journal of Remote Sensing* **26**:4999-5012

[8] Carrão Hugo, Gonçalves Paulo and Caetan Márioo 2008 Contribution of multispectral and multitemporal information from MODIS images to land cover classification *Remote Sensing of Environment* **112**:986-997

[9] Salami A T 1999 Vegetation Dynamics on the Fringe of Lowland Humid Tropical Rainforest of South-western Nigeria-an Assessment of Environmental Change with Air Photos and Landsat TM *International Journal of Remote Sensing* **20**:1169–1181

[10] Salami A T, Ekanade O and Oyinloye R O 1999 Detection of Forest Reserve Incursion in South-western Nigeria From a Combination of Multi-date Aerial Photographs and High Resolution Satellite Imagery *International Journal of Remote Sensing* **20**:1487–1497